

Sclerotic Vertebral Metastases: Pain Palliation Using Percutaneous Image-Guided Cryoablation

Ricardo Miguel Costa de Freitas · Marcos Roberto de Menezes · Giovanni Guido Cerri · Afshin Gangi

Received: 9 November 2010 / Accepted: 2 December 2010 / Published online: 18 December 2010
© Springer Science+Business Media, LLC and the Cardiovascular and Interventional Radiological Society of Europe (CIRSE) 2010

Abstract Cryoablative therapies have been proposed to palliate pain from soft-tissue or osteolytic bone tumors. A case of a patient with painful thoracic and sacral spine sclerotic metastases successfully treated by image-guided percutaneous cryoablation with the aid of insulation techniques and thermosensors is reported in this case report.

Introduction

Minimally invasive therapies, with curative or palliative intention, have taken place in the multidisciplinary approach of oncologic patients. Painful osteolytic metastases can be treated with percutaneous thermal ablative therapies, such as radiofrequency ablation (RFA) or cryoablation when other analgesic therapeutic options, such as opiate analgesia, chemotherapy, and radiation therapy, are ineffective or impractical [1].

Early impedance increase in sclerotic lesions RFA may result in an ineffective ablation zone [2]. Compared with

RFA limitations, cryoablation is not affected by the type of tissue and could theoretically be equally effective in treating osteolytic and sclerotic bone lesions [1]. To the current knowledge, this is the first technical report describing the case of a patient with two sclerotic spinal lesions that were successfully treated by image-guided percutaneous cryoablation.

Case Report

Institutional Review Board approval for retrospective case reports is not required by the institution where the procedure was performed. A 55-year-old woman with stage IV non-small-cell lung cancer presented moderate pain from sclerotic metastases at the thoracic and sacral levels (visual analog scores were 0.4 and 0.7, respectively). Pain at both levels was reproducible by palpation during physical examination. Computed tomography (CT) showed sclerotic lesions in the ninth thoracic vertebral body and at the left foramina margin of the second sacral vertebra (Fig. 1). The patient also presented chronic actinic pneumonitis and pericarditis and refused additional external beam radiation or opioid analgesic palliative treatment. After a multidisciplinary case review performed by pain specialists and interventional radiologists, percutaneous cryoablation was chosen as a minimally invasive therapy. Risks, benefits, and treatment options were explained to the patient, and informed consent was obtained.

Approach of the lesions was performed with the patient in prone position under general anesthesia and strictly aseptic technique. Percutaneous 10G needles (Optimed, Erlangen, Germany) were inserted under fluoroscopy and CT guidance. At the thoracic level, a 13G trephine (Cook, Bloomington, IN) was manually inserted through the 10G canula to create a

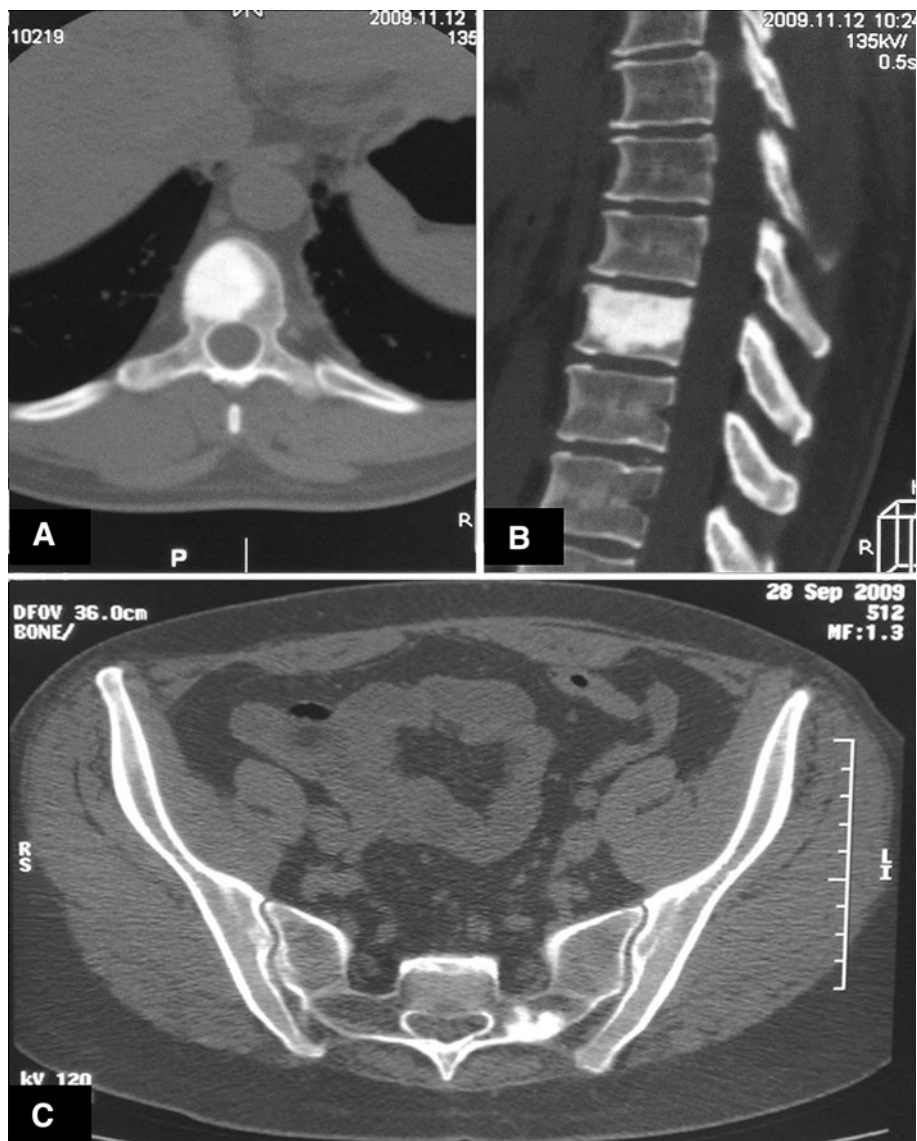
R. M. C. de Freitas (✉) · M. R. de Menezes
Department of Radiology, Instituto do Cancer do Estado de São Paulo, Avenida Doutor Arnaldo, 251 – Cerqueira César, São Paulo 01246-000, Brazil
e-mail: ricardomcfreitas@gmail.com

M. R. de Menezes · G. G. Cerri
Department of Radiology, Sírio Libanês Hospital, São Paulo, Brazil

G. G. Cerri
Department of Radiology, São Paulo University, São Paulo, Brazil

A. Gangi
Department of Radiology, Strasbourg University Hospital, Strasbourg, France

Fig. 1 CT of sclerotic bone metastases: axial (**A**) and sagittal (**B**) views of the ninth thoracic vertebra and axial view of second sacral vertebra (**C**)



pathway toward the center of the sclerotic lesion. A 1.7-mm diameter cryoprobe (Endocare, Irvine, CA) was then positioned inside the 10G needle (Figs. 2A, B, 3A). A 21G thermosensor (Endocare) inside an 18G needle was also inserted into the spinal canal to monitor temperature during cryoablation (Fig. 2B). A 22G spinal needle tip was positioned between the dural sac and the posterior wall of the vertebral body to allow displacement of the former by carbon dioxide (CO₂) injection (Figs. 2B, D). At the sacral level, the cryoablation probe was positioned at the lateral margin of the sclerotic lesion, away from the nerve root. A 22G spinal needle was positioned to displace the nerve root at the second left sacral foramina (Fig. 2D) as well as a thermosensor as previously described. Medical CO₂ was injected into the spinal canal through a two-step low-pressure closed CO₂ sterile system, adapted as described elsewhere [3, 4]. This system consists of a 4.5-l bottle of medical CO₂ (White

Martins, Rio de Janeiro, Brazil), delivered at 1.5 bars into a sterile drainage bag through a first stopcock. The bag was completely filled with CO₂ and, after turning the first stopcock, the gas was purged through a connecting tube to a second stopcock, which was connected with a Luer-lock 20-cc syringe. After closing the second stopcock, the CO₂ was then manually injected into the epidural space through another connecting tube attached to an antibacterial gas filter (Becton Dickinson, Juiz de Fora, Brazil) and then to the 22G spinal needle. CO₂ bag content was purged three times, before injection of the contents into the spine canal, to rid the injection system of room air. Injection of CO₂ was monitored by fluoro-CT (Fig. 3B). A 10-min cycle of freezing was performed followed by 10-min active thawing. Temperature at thermosensors reached 22°C into the spinal canal at the thoracic level and 11°C at the sacral level. CT monitoring did not show a change in density of the paravertebral tissues.

Fig. 2 Intercostovertebral approach of the ninth thoracic (T9) vertebra, lateral fluoroscopy view (**A, B**): 13G trephine inside the 10G needle (**A**) and 22G needle (**filled arrow**) for CO₂ injection and an 18G needle (**open arrow**) for the thermosensor (**B**). Metallic artifact projection at T9: sphygmomanometer at the left arm (**B**). Axial CT: 22G needle tip at the anterior epidural T9 space filled with CO₂ (**C**) and a 22G needle tip and CO₂ at the periradicular sacral space (**D**)



The needles were removed, and the patient was sent to the recovery room. There were no complications during or immediately after the procedure. No medications for pain were requested after treatment, and the patient was discharged the next day from hospital without complaints.

An MRI study performed 30 days after the procedure showed minor changes inside the sclerotic lesion in the ninth vertebral body (Fig. 3C, D) and alterations in the lateral aspect of the sacral lesion, but no signal abnormalities were noted in the nerve root or within the epidural space of S2 left foramina (Fig. 4). The patient survived another 5 months after the procedure and she did not complain of bone pain or develop any complication related to the cryoablation treatment. The progression of intrathoracic nodal involvement eventually led her to death.

Discussion

Metastatic bone lesions, which are usually amenable to ablative therapy, are typically either osteolytic or mixed osteolytic/osteoblastic in nature and otherwise composed of soft tissue [2]. A successful palliative treatment with cryoablation of painful sclerotic bone metastases located in the spine is reported in this article.

Cryotherapy is the oldest ablation method with less peri and postprocedural pain. New miniaturized argon-gas devices create an “ice-ball” and induce cellular necrosis at lower than -20°C [1, 5]. The “ice ball” can be formed deeply in bone, whereas RF ablation is poorly delivered into sclerotic or otherwise intact bone due to early impedance increase [6, 7]. Treatment of sclerotic bone metastases with cryoablation was considered technically feasible, although it was usually taken for as an excluding criteria due to difficulties in accessing sclerotic bone or because sclerotic metastases are often multifocal whenever present. As a general guideline, another exclusion criteria reported when dealing with patients with spinal bone metastases is the treatment of a portion of the lesion located within 1 cm of the spinal cord, major motor nerve, or artery of Adamkiewicz, unless insulating techniques are available [2, 8]. Thermal ablation may jeopardize the spinal canal structures when protective measures are not available [9]. The treatment of a patient with two major painful sclerotic vertebral lesions was considered feasible. To protect nerve structures, we adopted the same technique as described elsewhere to treat osteolytic spinal lesions, i.e., insulating technique with CO₂ injection at the epidural space, monitoring the temperature at the spinal canal with thermosensors, and using CT-imaging guidance [4].



Fig. 3 **A** Axial CT showing cryoprobe (white arrow) inserted in the ninth thoracic (T9) vertebra metastasis and **B** insulation of dural sac with CO_2 (black-outlined open arrow) at the anterior epidural space.

C Axial T1WI MR of T9 with diffuse hypointensity of the sclerotic metastasis before treatment and **D** mild hyperintensity (open arrowheads) covering the area of cryoablation 30 days after treatment

Several mechanisms of pain from bone metastases can be listed: direct metastatic bone invasion with microfractures; increased pressure on endosteum and distortion of periosteum; nerve-root compression or muscle spasm in the lesion area; and release of chemical mediators involved in the conduction of nociceptive impulses to the central nervous system [1, 10]. In addition, osteoclastic bone resorption also plays a role to the pathophysiology of osteoblastic metastases [11]. Otherwise, the primary goal of symptomatic pain relief when treating osteolytic bone metastases with thermal ablative techniques is to ablate the interface between the tumor and the pain-sensitive periosteum [2]. The exact mechanism why cryoablation can relieve pain from sclerotic bone metastases remains elusive. The cancerous cell burden, the higher endosteum pressures, or the release of pain-related chemical mediators may all influence pain intensity in sclerotic metastases.

Imaging criteria to select and follow-up patients should include the fact that bone produced in response to tumor cells can be weak and fragile although it appears sclerotic on plain X-ray. A report on histopathology analysis of sclerotic reaction to prostate bone tumors showed that the lesions were composed mostly of woven bone with small

amounts of osteoid and native bone trabeculae appearing as a lamellar bone. Despite an increase in average bone volume, only half of the sclerotic metastases were osteodense in that study [12]. Several patients also present changes in metastatic bone appearance after chemotherapy or radiotherapy [13]. The imaging analysis of candidates to spinal sclerotic bone cryoablation should consider these issues because thermal ablation therapies could also induce transient tissue weakness in the first hours or days after treatment. In some cases, the use of this technique alone may increase the risk of fractures and thus is not suitable for weight-bearing bones.

In this case report, a shorter cryoablation freezing cycle was chosen during treatment planning with the intent to promote partial necrosis of the sclerotic lesions and to achieve pain relief without compromising vertebral stability or neural structures. According to Callstrom et al. [5], cell death from cryoablation is due to two causes. First, rapid freezing immediately adjacent to the probe results in intracellular ice formation and subsequent cell destruction. At a further distance from the probe, relative gradual cooling causes osmotic differences across the cell membrane, with secondary cellular dehydration and death [5].

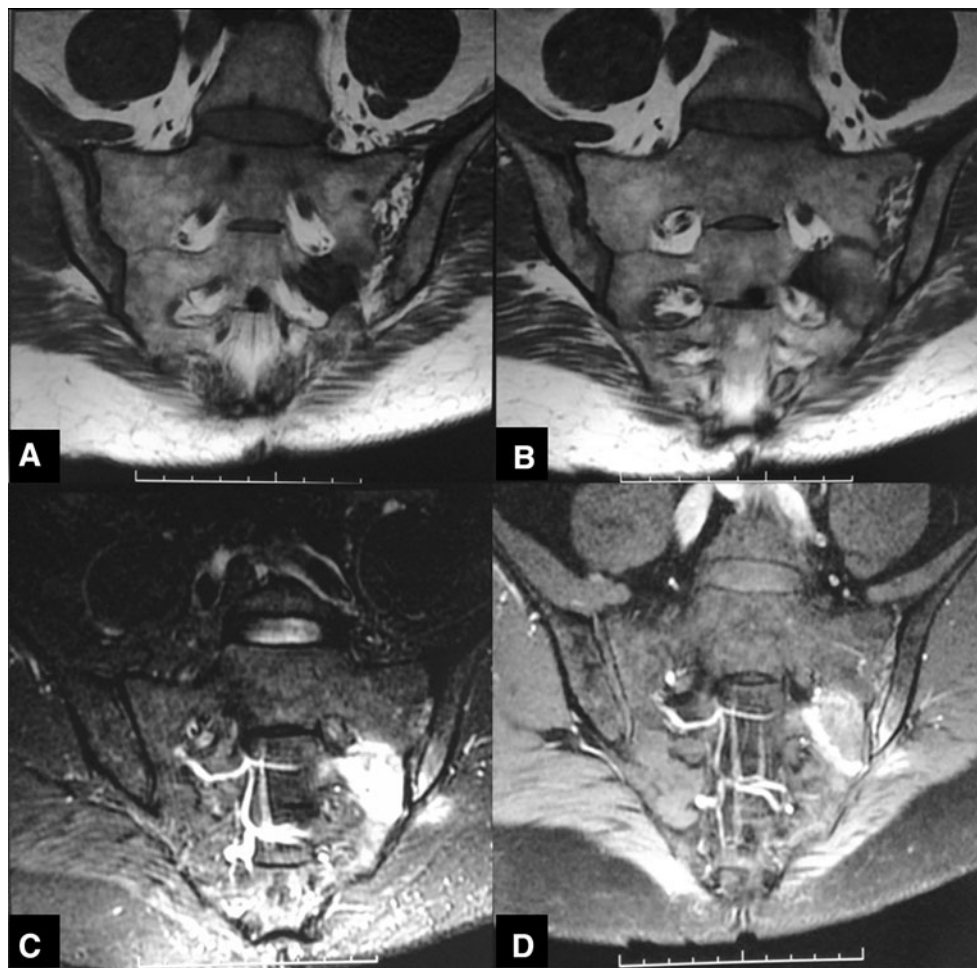


Fig. 4 Coronal MR of the sacrum. **A** Bone lesion with T1WI hypointensity at left second sacral (S2) vertebra. **B** Hypointensity halo of the treated area on T1WI partially covering the sclerotic bone

lesion and normal bone. **C** Hyperintensity on T2WI and **D** hyperintensity halo with mild central enhancement on T1WI C+

Given relative cellular tolerance to freezing temperatures, complete cell death occurs within approximately 3 mm internal to the “ice-ball” margin. Shorter or longer freezing times are employed depending on the adequacy of coverage of the lesion and the proximity of adjacent critical structures [2]. We then performed one cycle of 10-min freezing to limit the extension of cryoablation, expecting a 1.4 cm diameter isotherm of -40°C . This amount of frozen tissue would fit into the edges of the thoracic vertebral sclerotic lesion and would be limited to at least the lateral half of the sacral lesion. “Ice-ball” formation can be actively monitored by CT while decreasing soft-tissue density can be seen. Its size varies depending on the length of uninsulated tip, on the volume of gas passing through the probe, and on the time of freezing. No change in density within a sclerotic bone lesion is expected during cryoablation–CT monitoring, but it would be possible to see progression of freezing with surveillance of the neighboring paraspinal soft tissues, which was not seen in the present

case. Thermosensors did not display a temperature decrease $<10^{\circ}\text{C}$ into the spinal canal, and CO₂ epidurography performed during the freezing cycle warranted additional protection to the spinal cord and its nerve roots.

Cryoablation is a feasible technique to palliate pain caused by sclerotic bone metastases in the spine and can benefit a set of patients who are not amenable to usual therapies. Further investigation on clinical and imaging criteria to select and follow-up patients is required to validate this technique.

Conflict of interest The authors declare that they have no conflict of interest.

References

1. Sabharwal T, Katsanos K, Buy X et al (2009) Image-guided ablation therapy of bone tumors. *Semin Ultrasound CT MRI* 30:78–90

2. Callstrom MR, Charboneau JW (2007) Image-guided palliation of painful metastases using percutaneous ablation. *Tech Vasc Interv Radiol* 10:120–131
3. Chao A, Major K, Kumar SR et al (2007) Carbon dioxide digital subtraction angiography-assisted endovascular aortic aneurysm repair in the azotemic patient. *J Vasc Surg* 45:451–460
4. Buy X, Tok CH, Szwarc D et al (2009) Thermal protection during percutaneous thermal ablation procedures: interest of carbon dioxide dissection and temperature monitoring. *Cardiovasc Interv Radiol* 32:529–534
5. Callstrom MR, Charboneau JW, Goetz MP et al (2006) Image-guided ablation of painful metastatic bone tumors: a new and effective approach to a difficult problem. *Skeletal Radiol* 35:1–15
6. Dupuy DE, Hong R, Oliver B et al (2000) Radiofrequency ablation of spinal tumors: temperature distribution in the spinal canal. *AJR Am J Radiol* 175:1263–1266
7. Callstrom MR, Atwell TD, Charboneau JW et al (2006) Painful metastases involving bone: percutaneous image-guided cryoablation—prospective trial interim analysis. *Radiology* 241:572–580
8. Callstrom MR, York JD, Gaba RC et al (2009) Research reporting standards for image-guided ablation of bone and soft tissue tumors. *J Vasc Interv Radiol* 20:1527–1540
9. Nour GS, Aschoff AJ, Mitchell ICS et al (2002) MR imaging-guided radio-frequency thermal ablation of the lumbar vertebrae in porcine models. *Radiology* 224:452–462
10. Mercadante S, Fulfaro F (2007) Management of painful bone metastases. *Curr Opin Oncol* 19:308–314
11. Guise TA, Mohammad KS, Clines G et al (2006) Basic mechanisms responsible for osteolytic and osteoblastic bone metastases. *Clin Cancer Res* 12(20 Suppl):6213s–6216s
12. Roudier MP, Morrissey C, True LD et al (2008) Histopathological assessment of prostate cancer bone osteoblastic metastases. *J Urol* 180:1154–1160
13. Du Y, Cullum I, Illidge TM et al (2007) Fusion of metabolic function and morphology: sequential [¹⁸F] fluorodeoxyglucose positron-emission tomography/computed tomography studies yield new insights into the natural history of bone metastases in breast cancer. *J Clin Oncol* 25:3440–3447